PB-FHR Reserve Shutdown System

Shuokai Chang, Abel Gonzalez, Justin Kong, and Nick Satterlee
University of California, Berkeley
Department of Nuclear Engineering

Report UCBTH-12-008

May 4, 2012

ABSTRACT

This report describes a reserve shutdown system for Pebble Bed Fluoride-salt cooled high temperature reactors (PB-FHRs) that utilize neutron absorbing blades inserted into the pebble core in locations with high neutron flux. When triggered, the reserve shutdown rods are embedded into the pebble bed core by their own weight to depths that greatly reduce the core reactivity and shutdown the reactor.

CONTENTS

1.0 INTRODUCTION

The Pebble-Bed Fluoride Salt Cooled High Temperature Reactor (PB-FHR) uses buoyant rods for normal shutdown (Blandford, 2008). These rods, which are neutrally buoyant at 615°C, will drop into the reactor core when the coolant temperature in the shutdown channel increases above the normal value of 600°C, or when a reactor scram occurs and forced insertion is activated.

For safety, the PB-FHR must also have a redundant and diverse system for reserve shutdown. This project studied several options for reserve shutdown, and selected, designed, and tested a system using specially-designed cruciform shutdown blades driven directly into the pebble bed by gravity.

1.1 Rods or Spheres

There are various methods of implementing reserve shutdown systems in nuclear reactors, but many require time-consuming maintenance after activation such as soluble poisons or neutron absorbing pellets. Two alternative systems were observed that can be easily reset after activation with minimal maintenance. The first system considered consists of neutron absorbing spheres and a cylindrical channel. The spheres are held in a hopper during normal reactor operation, but, when triggered, they fall into the channel and absorb neutrons. The second system considered involves reserve shutdown rods being inserted directly into the pebble-bed core without aid of a channel.

The reserve shutdown rods inserted into the pebble core are chosen for the reserve shutdown system in lieu of spheres because reserve rods share fewer design features with the standard shutdown system (which uses a buoyant rod in a shutdown channel), reducing the probability of a common mode failure. Like the buoyant rods used for normal shutdown, shutdown spheres require dedicated channels for insertion. These channels can only be accommodated by displacing normal shutdown rods or creating new channels in the core.

The fact that spheres need the same type of channels as do the normal shutdown rods will likely increase risk by reducing the diversity of the reactivity control systems, and the latter requires constructing a channel that must withstand high neutron fluence as well as constant forces imposed by the spheres, while being thin enough to maintain significant neutron transparency. Furthermore, a reserve system that utilizes the same method of transportation to the core as the standard shutdown rods (buoyant insertion into a cylindrical channel) is at risk of failing from common cause, e.g. if an earthquake disables normal shutdown rod channels it may also disable reserve channels as well.

The drawbacks inherent in using channels for the insertion of spheres do not plague the alternative option of cruciform reserve shutdown rods. The rods are positioned above the active region of the core and, when released, insert directly into the pebble bed, sliding through the fuel pebbles to reach the high flux region of the core. Thus, the rods are not at risk of affecting reactivity during normal operation, but will quickly and efficiently reduce reactivity after insertion.

1.2 Project Goals

To ensure high reliability of the reserve shutdown system: the blades are to be inserted into the pebble bed core under their own weight; the blades must be fully inserted within a reasonable amount of time (to be determined); the blades and the displaced fuel pebbles should not break during insertion; corrosion of the blades must be insignificant during the lifetime of the plant; upon insertion they must be able to bring the core to subcriticality; the core is to remain subcritical during long term shutdown even after xenon decays away; and subcriticality must be achieved even in the event one of the blades fails to insert.

These goals must be accomplished within the given design constraints of the project: the blades width must be under half the diameter of a sphere to avoid fuel pebbles entering the rod insertion channels above the core; the length of the blade must be six sphere diameters; the blade cannot be closer than four sphere diameters to the defueling chute to maintain mechanical integrity; and the length and width of the flanges must be at most half a sphere diameter to avoid pinning of fuel pebbles during defueling.

To accomplish these goals under the given design constraints, the geometry and material composition of the blades will be designed to satisfy all the parameters. The geometry and materials, insertion time, neutronics and mechanical integrity of the blades and fuel pebbles will be varied to best fit the system. The blade tip can be designed to minimize the force necessary to insert the rod and to minimize the potential for damage or cracking of fuel pebbles. The cladding material and thickness will also be selected to ensure the blades do not fracture during insertion, and so the selected material experiences minimal corrosion in the implemented environment. The materials and geometry of neutron poison in the center of the blade will be selected to ensure sufficiently high neutron capture probability.

2.0 NEUTRONICS (Nick Satterlee)

Neutronic analysis was performed using two methods: approximate analytical solutions and and simulation of the activated reserve system implemented in the full core with MCNP5. The approximations were used during design of the rods to ensure the rods absorb a significant percentage of incident neutrons.

The effectiveness of the reserve shutdown system was verified by modeling the reserve system using Monte Carlo simulation. The reserve system was adapted into the steady-state PB-FHR Test Reactor model and simulated with MCNP5 for varied cladding thicknesses. The Test Reactor is a small, 20-MWth core design being studied that has a total core volume of approximately 1 m^3. This initial MCNP analysis was used to determine the maximum support cladding of the reserve shutdown rod. Subsequent simulations determined the number of reserve rods necessary to achieve and maintain subcriticality without aid of the buoyantly activated normal shutdown rod system or control rods.

2.1 Neutronic Approximations

Before attempting the time intensive Monte Carlo simulations, a brief analytical calculation was made to verify the feasibility of the design given the constraints of natural boron and a blade

width less than the radius of a fuel sphere (1.5cm). The width reduction was considered because structural cladding must be included around the central absorbing region to maintain structural integrity of the rod when it is inserted into the core and provide corrosion protection from the reactor coolant. Because the clad must surround the entire absorbing region, a 0.1cm increase in cladding width results in a 0.2cm reduction in the thickness of the center absorbing region.

The analytical approximation estimates the probability of a single neutron with thermal, epithermal, and fast energies passing through a slab of boron-carbide of natural isotopic composition without an absorption interaction. The neutron is assumed to be incident normal to the slab surface for conservative analysis. For this simple approximation, the design was considered feasible if the neutron escape probability is less than 1% (absorption probability > 99%).

The slab is approximated by infinite height and length with variable width depending on the absorber thickness. The cladding is assumed to be transparent to neutrons and thus is not included in the calculation. The total absorption cross section tabulated in Table 2.1 and atom density of B_4C tabulated on Table 2.2 were used to compute the neutron capture probabilities in Table 2.3 with the equation:

$$P_{escape}(\Delta x, E_n) = e^{-\sigma N x \Delta} \qquad 1)$$

Equation (1) assumes an infinite B_4C slab with finite width Δx, absorption cross section, σ, and atom density N. Because cross sections are highly dependent upon neutron energy, the probability was evaluated for thermal, epithermal and fast neutron energies.

Table 2.1: Tabulated absorption cross-sections for natural B_4C. Total values were obtained by weighting isotopic concentrations. Total cross-sections are subject to +/- 4% error.

E (MeV)	2.53E-08	1.0E-06	1.0E-05	1.0E-04	1.0E-03	0.1	1
^{13}C XS (b)	1.37E-03	2.13E-04	6.89E-05	2.07E-05	6.63E-06	2.73E-05	5.29E-07
^{12}C XS (b)	3.37E-03	5.35E-04	1.68E-04	5.35E-05	1.71E-05	9.00E-07	1.31E-06
^{10}B XS (b)	3845.16	598.15	193.02	60.22	21.14	4.86	2.31
^{11}B XS (b)	5.50E-03	8.66E-04	2.65E-04	8.59E-05	2.77E-05	2.50E-06	2.26E-06
Total	**612.15**	**95.23**	**30.73**	**9.59**	**3.37**	**0.77**	**0.37**

Table 2.2: Calculation of the atomic mass with natural isotopic composition of Boron.

Natural concentration	Atomic Mass (g/mol)	Atom percent
^{12}C	12.0000000	0.19786
^{13}C	13.0033548378	0.00214
^{10}B	10.0129370	0.1592
^{11}B	11.0093055	0.6408
Total	**11.05016**	1
B_4C Density (g/cm3)	**2.52**	
Atom density (#/cm3)	**1.37332E+23**	

Table 2.3: Probability for a neutron of various energies, normal to the slab, escaping without being captured. Bold entries indicate the approximate maximum energy neutrons that can be absorbed with high confidence ($P_{escape} < 0.01$).

Δx (cm)	**P(Thermal)**	**P(1e-6 MeV)**	**P(1e-5 MeV)**	**P(1e-4 MeV)**	**P(1e-3 MeV)**	**P(0.1 MeV)**	**P(1 MeV)**
1.5	2.30E-55	3.02E-09	**1.78E-03**	0.139	0.500	0.853	0.927
1.3	4.44E-48	4.14E-08	**4.14E-03**	0.181	0.548	0.871	0.937
1.1	8.56E-41	5.66E-07	**9.64E-03**	0.235	0.601	0.890	0.946
0.9	1.65E-33	**7.73E-06**	0.0224	0.306	0.660	0.909	0.956
0.7	3.18E-26	**1.06E-04**	0.0521	0.398	0.724	0.928	0.965
0.5	6.13E-19	**1.45E-03**	0.121	0.518	0.794	0.948	0.975
0.3	**1.18E-11**	0.0198	0.282	0.674	0.871	0.969	0.985
0.1	**2.28E-04**	0.270	0.656	0.877	0.955	0.989	0.995

The data tabulated on Table 2.3 and plotted on Figure 2.1 shows that for any thickness, natural boron isotopic concentrations are appropriate for thermal neutrons. Escape probabilities greatly increase for epithermal neutrons: for 1E-6 MeV, the width should not be less than 0.3cm; for 1E-5 MeV, the width should not than 1.1cm; and for energies greater than 1E-5 MeV, the natural B_4C no longer maintains high confidence for any width.

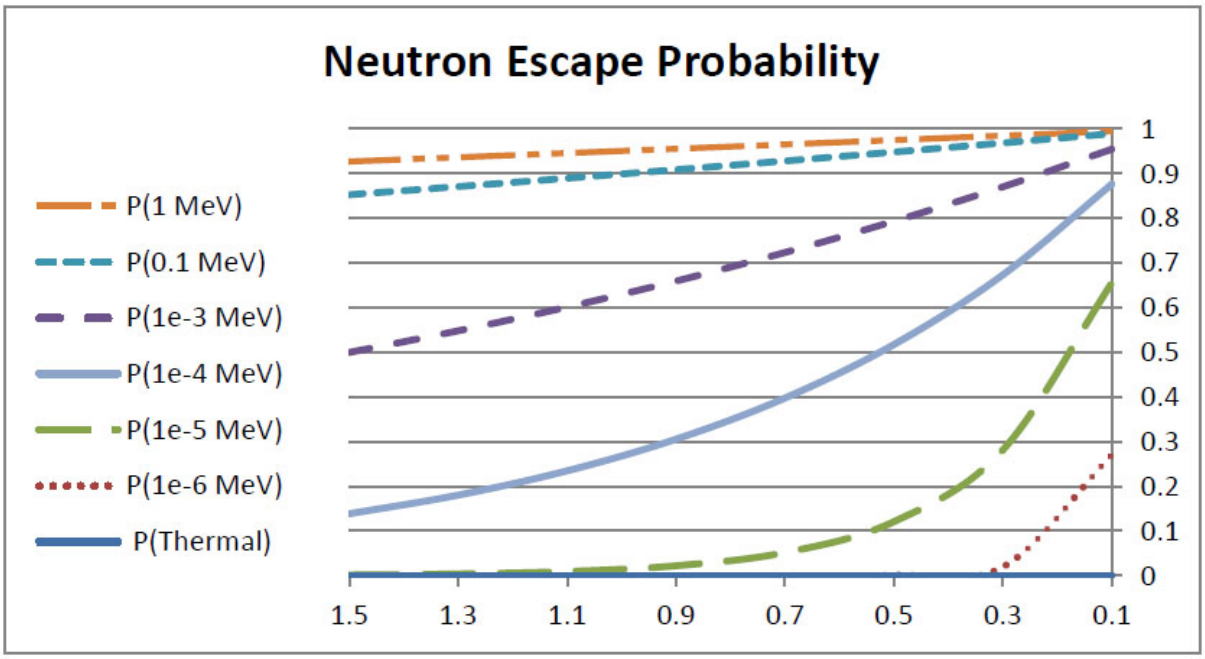

Figure 2.1: Escape probability for a single neutron of various energies plotted from Table 2.2

Because the rod is inserted directly into the core, the neutron energy spectrum is expected to significantly exceed thermal energies. Table 2.3 indicates that any width is acceptable as long as the proposed cladding and B_4C provide sufficient neutron moderation. Elastic and inelastic scattering, ignored in this calculation, should provide some moderation within the B_4C absorber. If moderation and absorption from the structural cladding around the B_4C absorbing region is also considered, the escape probabilities could be significantly lower than the calculated approximations.

For cladding greater than 0.6cm (and the B_4C absorbing region in the center of the rod less than 0.3cm), neutrons should be moderated to near-thermal energies within the B_4C region. If cladding must consume 0.3cm to 0.5cm (and the B_4C region 0.9cm to 0.5cm respectively), neutrons should be moderated to approximately less than 1E-06 MeV. For clad thicknesses less than 0.2cm, neutrons should be moderated to energies around 1E-05 MeV. These results appear to be reasonable despite their conservative derivation, hence natural boron will initially be considered for MCNP calculation.

2.2 MCNP Simulation

MCNP simulations were carried out by modeling a rod with a width of six pebble diameters (15cm) and thickness of half a pebble diameter (1.5cm), inserted into a small FHR Test Reactor core with a total volume of approximately 1 m^3. The height of the rod was modeled as the distance from the top of the converging to the top of the defueling chute (157cm). This height was chosen so the entire volume of the rod could be conserved during insertion tests, because histories of neutrons escaping from the top of the chute are terminated. Figure 2.2 displays the MCNP5-generated image of the fully inserted rod in the reactor core.

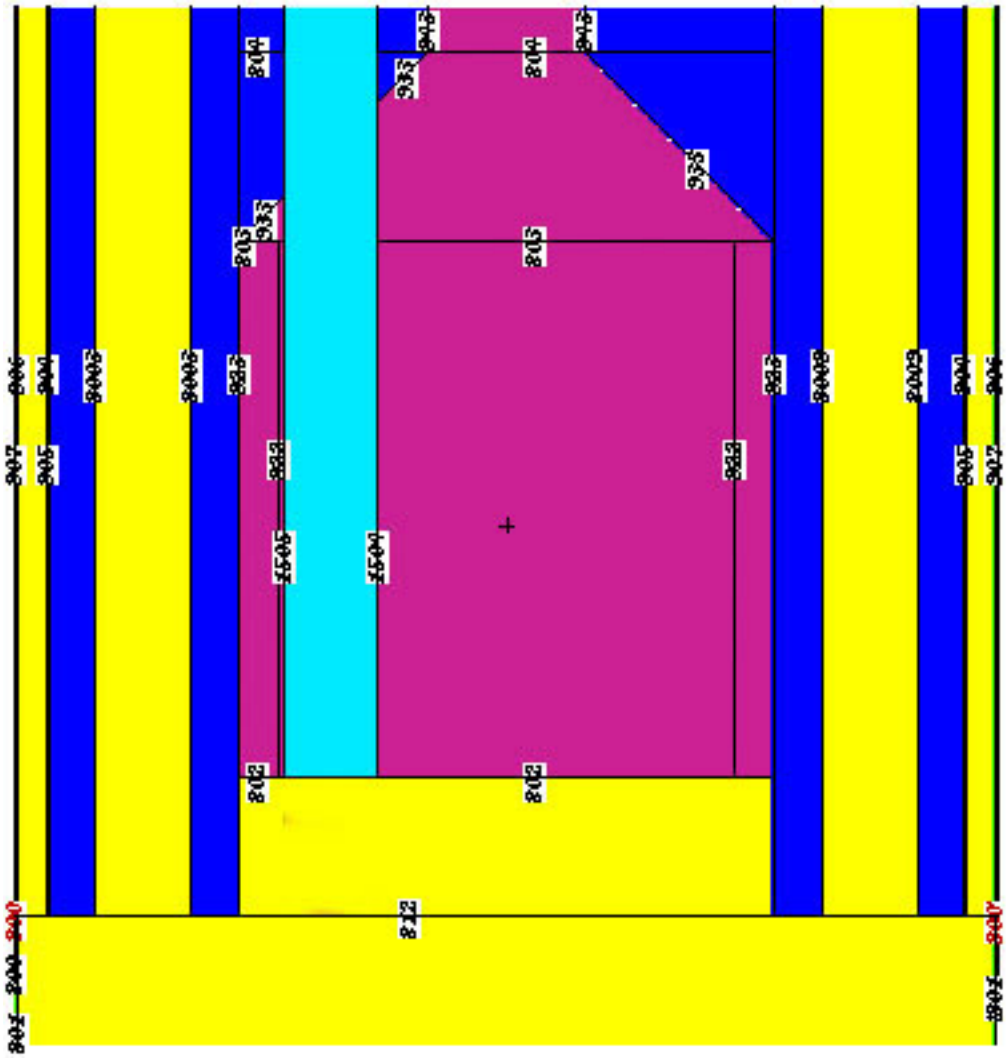

Figure 2.2: Diagram of the insertion rod in the reactor core. Light blue represents the inserted rod, dark blue denotes the graphite reflecting regions, pink represents the area occupied by fuel pebbles, and yellow regions are inhabited solely by coolant. The entire defueling chute is not displayed.

2.2.1 Single Rod Test

Initial simulations performed with MCNP5 were used to verify the effectiveness of the reserve shutdown system with varying cladding thicknesses. The cladding provides mechanical and corrosion protection to the B_4C residing within the rod, and thus cladding thickness is integral to the mechanical stability of the reserve rods during insertion.

Simulation of the rod was carried out by homogenizing the boron-carbide and cladding and varying the isotopic density and concentration in each case. The element ratios for each rod are tabulated on Table 2.4, each element is assumed to be of natural isotopic concentrations. Isotopic concentrations and densities were computed by weighting the natural values for each material with the corresponding volume ratios.

Table 2.4: Tabulation of element concentrations and boron isotopic concentrations for each cladding thickness.

Clad Width	**0.1cm**	**0.2cm**	**0.3cm**	**0.4cm**	**0.5cm**	**0.6cm**	**0.7cm**
B-10	1.36E-01	1.14E-01	9.23E-02	7.10E-02	5.01E-02	2.97E-02	9.79E-03
B-11	5.49E-01	4.59E-01	3.72E-01	2.86E-01	2.02E-01	1.20E-01	3.94E-02
C	1.71E-01	1.43E-01	1.16E-01	8.93E-02	6.31E-02	3.75E-02	1.25E-02
Ti	7.15E-04	1.41E-03	2.10E-03	2.77E-03	3.43E-03	4.07E-03	4.69E-03
Zr	1.14E-04	2.26E-04	3.36E-04	4.43E-04	5.48E-04	6.51E-04	7.51E-04
Mo	1.42E-01	2.81E-01	4.17E-01	5.51E-01	6.81E-01	8.08E-01	9.33E-01

To determine the effectiveness of natural boron, MCNP simulation of the fully inserted rods was completed with MCNP5 and compared with an ideal absorbing rod. The ideal rod was simulated with a perfect neutron absorber by terminating the histories of any neutrons entering the rod geometry. The reactivity of each system was compared to the ideal system in order to determine the effectiveness of natural boron for all possible design scenarios. Equation 2) was used to determine the percent worth of each rod.

$$\% \, max \, worth = \frac{\rho clad}{\rho ideal} = \frac{Rideal(Rclad-1)}{Rclad(Rideal-1)} \qquad 2)$$

where ρ_{clad} is the reactivity of a rod with a given cladding width, ρ_{ideal} is the reactivity of the ideal rod inserted into the core. The percent of the maximum possible worth for each rod is graphed on Figure 2.3 by use of Equation 2).

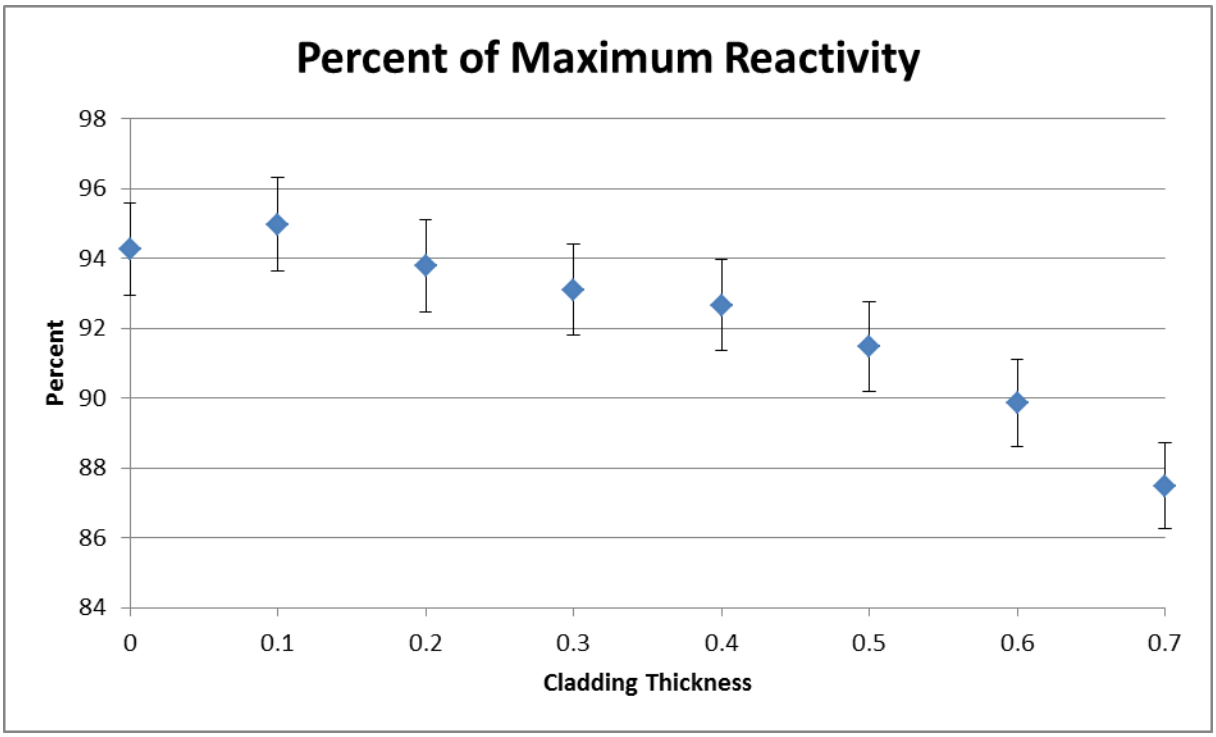

Figure 2.3: Percent of maximum possible reactivity for each rod with varying cladding thicknesses.

Figure 2.3 shows that natural boron enrichment comes close to a perfect neutron absorber. This simulation confirms that natural boron enrichment will be appropriate for the reserve shutdown rod. MCNP simulation for insertion tests will assume a cladding thickness of 0.5cm for conservative results.

2.2.2 Insertion Tests

The reserve shutdown system requires the shutdown blades to the inserted into the reactor core. In order to determine the minimum insertion depth required to achieve and maintain subcriticality, K_{eff} was evaluated for eleven equally spaced insertion depths from 0% to 100% of the core and converging cone height. Figure 2.4 displays the simulation depths of the insertion blades.

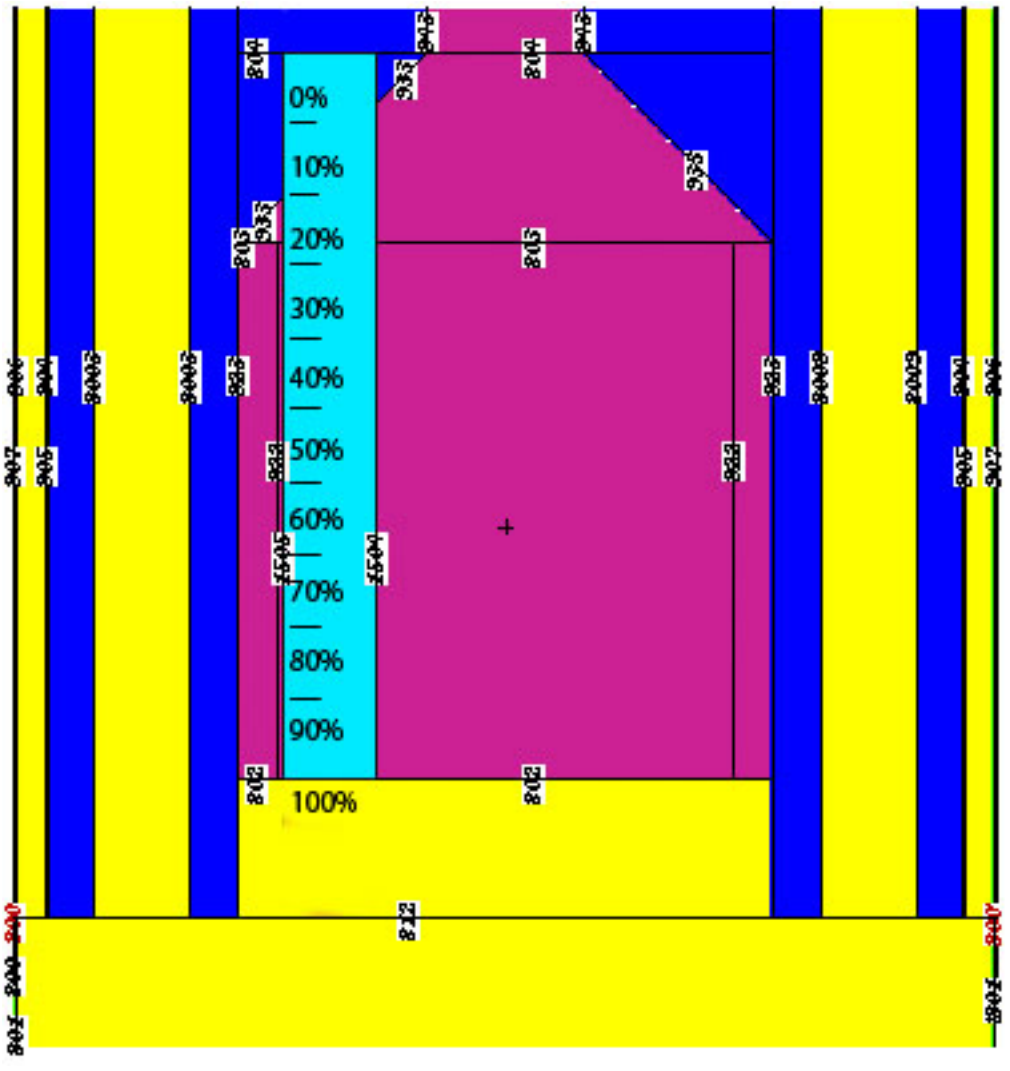

Figure 2.4: Insertion depths evaluated during simulations. Maximum depth at 100% is full insertion and minimum depth at 0% represents a rod stopped in the top of the converging cone.

The test was conducted for two, three and four rod systems. For conservative results, one rod in each test was assumed to fail; hence, the two rod system was evaluated for one rod, the three rod system was evaluated for two rods 120^{o} apart and the four rod system was evaluated for three rods spaced 90^{o} apart.

Figure 2.5 displays the insertion test for a two rod system. Because it is assumed one rod will fail in each test, this can also be considered a single rod success. It is observed that the maximum reactivity worth is achieved with approximately 70% insertion. After 70% insertion, K_{eff} remains constant at 0.9787 +/- .0006. It is expected that if a longer rod were used, that would extend further above the core, then K_{eff} would continue to drop until 100% insertion is reached.

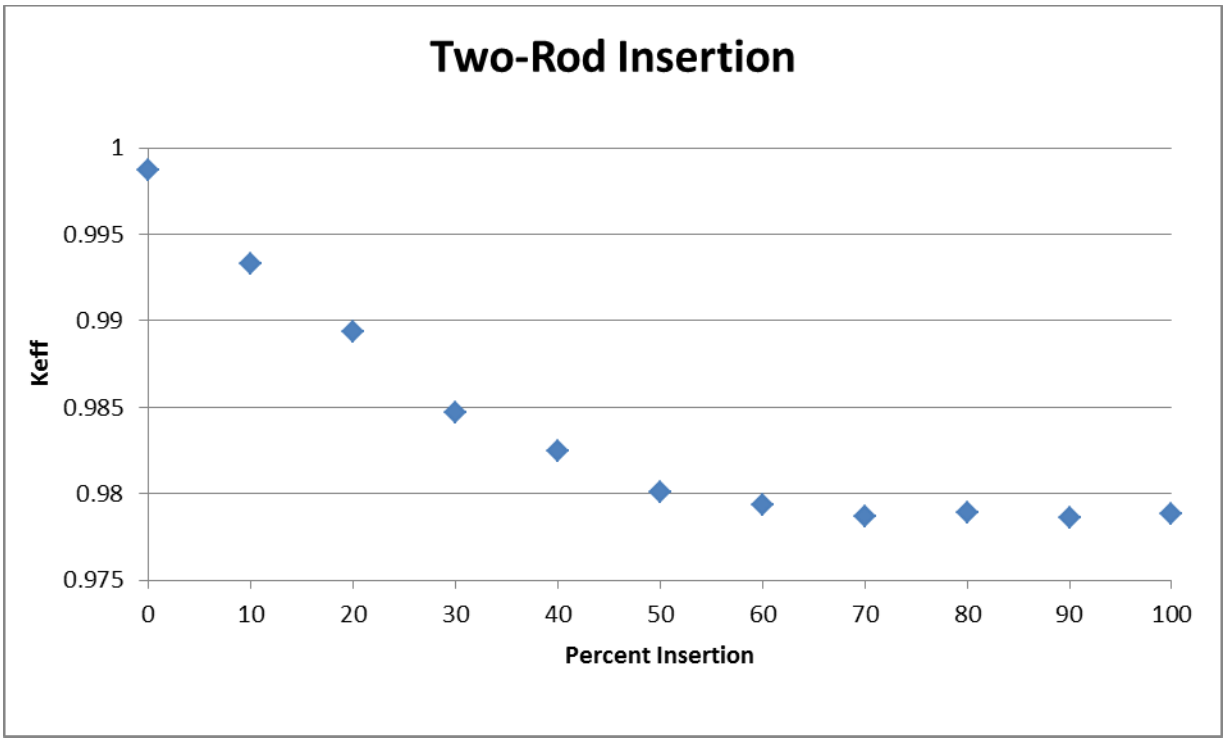

Figure 2.5: Two Rod system with a single rod failure. Error bars not plotted because they are too small to be resolved.

The three-rod system presented in Figure 2.6 displays a similar trend to the two rod system. The maximum K_{eff} once again converges at about 70% insertion with a value of 0.9576 +/- 0.0006

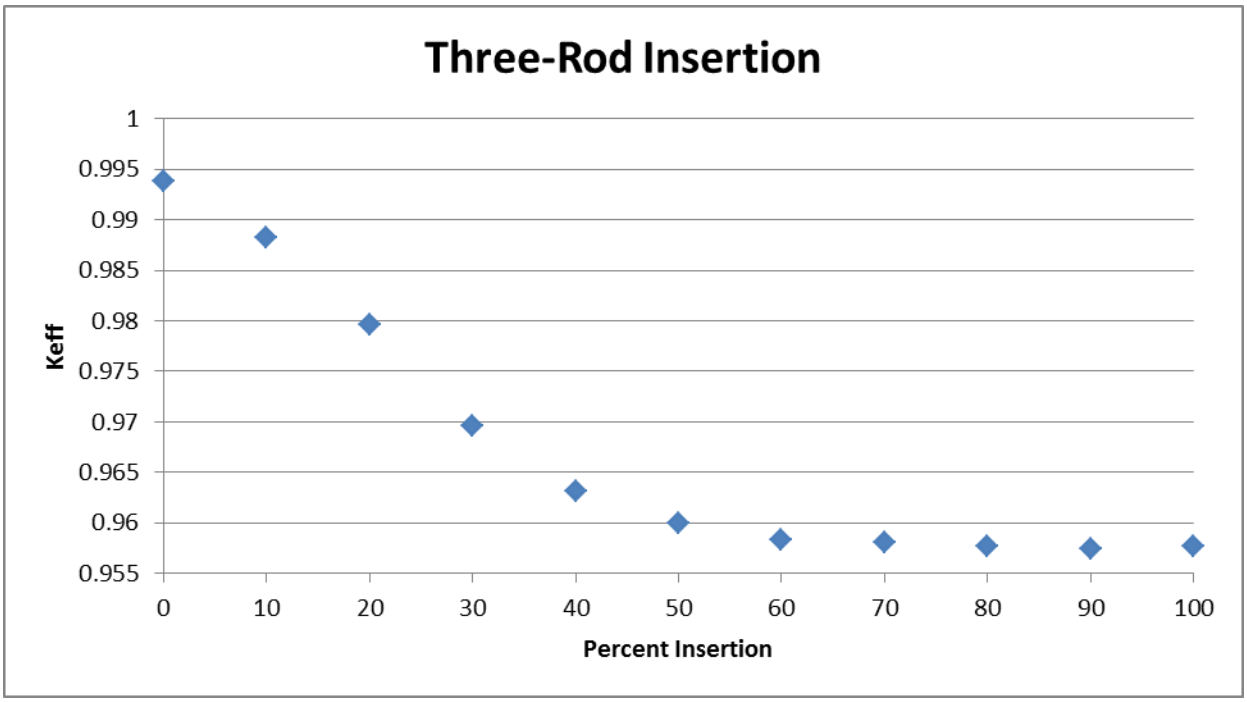

Figure 2.6: Three rod system with a single rod failure. Error bars are too small to be resolved.

The four-rod system presented on Figure 2.7 maintains the trend of maximum worth at a depth of 70% with a K_{eff} of .9397 +/- .0006; further insertion does not change the K_{eff} of the system.

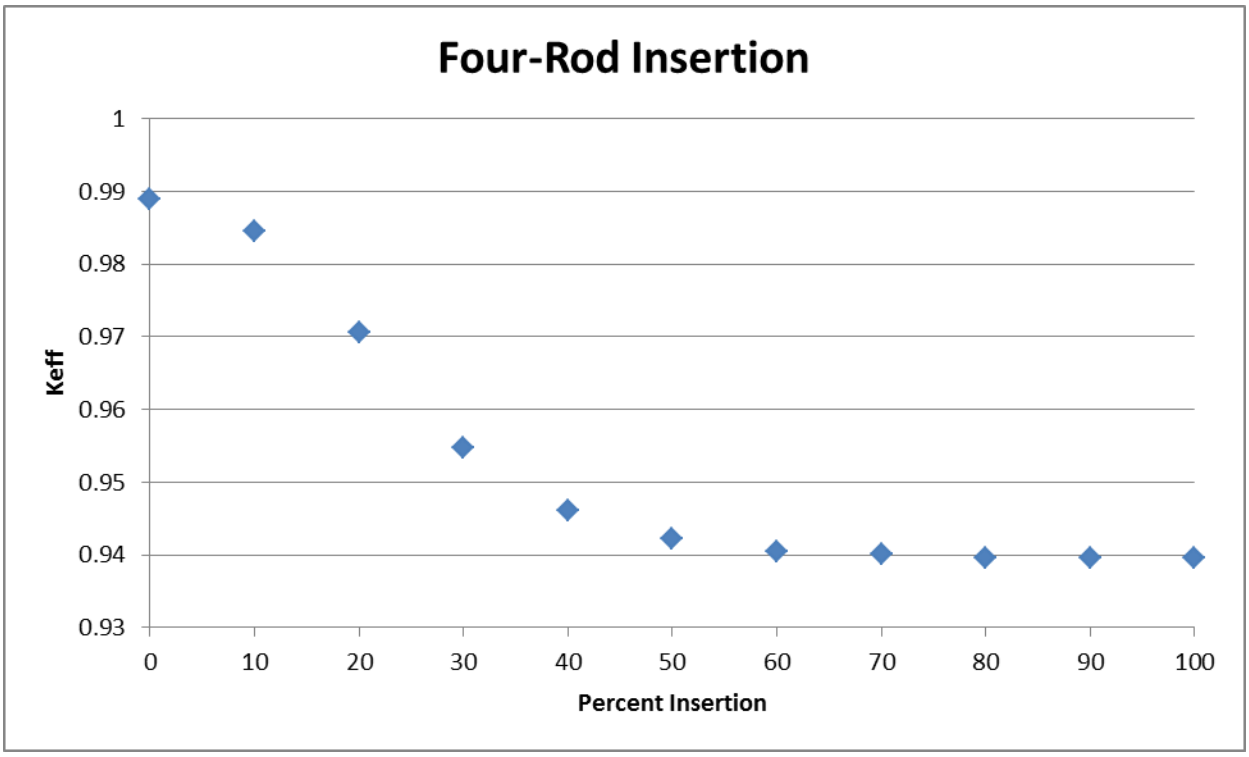

Figure 2.7: Four-rod insertion system with a single rod failure. Error bars are too small to resolve.

The primary difference in each insertion test is the K_{eff} trend at small insertion depths. With the addition of each rod, the slop at small depths decreases. Figure 2.8 displays the trend for each system. The addition of each rod decrease the reactivity of the system in a linear manner, but K_{eff} is defined as $1/(1-\rho)$. Thus, K_{eff} is predicted to decrease in smaller increments with the addition of each rod. These results should also exacerbate the trend because the single rod failure results in uneven rod distribution.

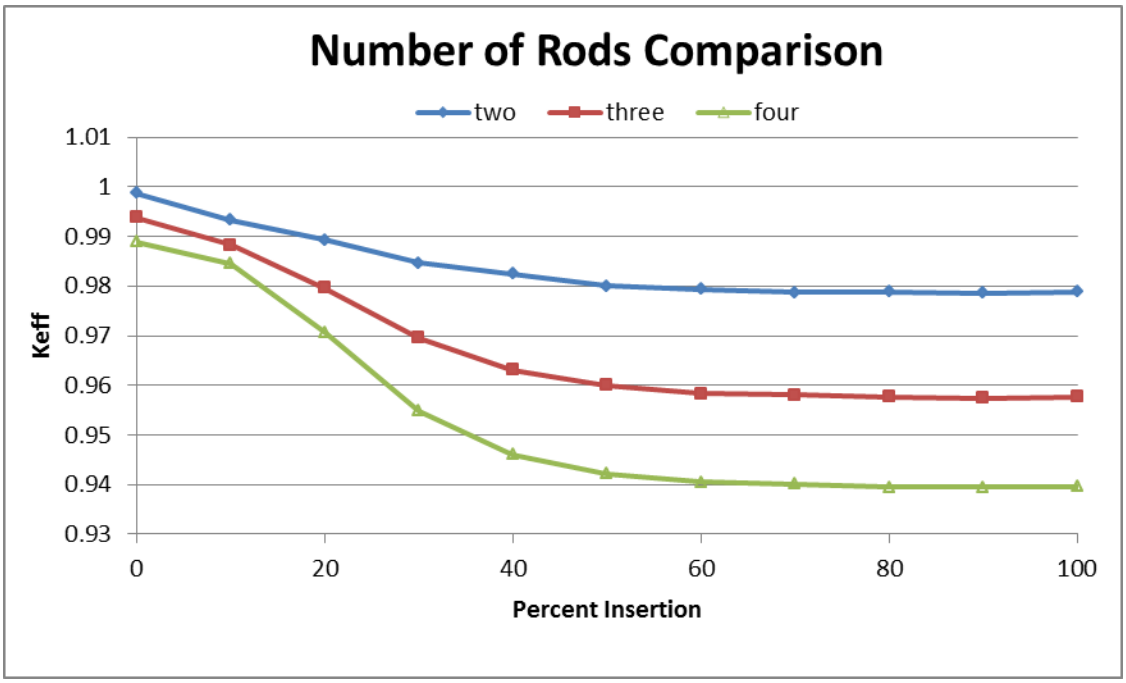

Figure 2.8: Comparisons of number of rods inserted with a single failure.

The insertion tests concluded that the maximum reactivity worth of the rod can be achieved with 70% depth insertion. The next evaluation was carried out to determine the number of rods required to maintain shutdown over long periods of time.

2.3 Cold Shutdown Requirements

To maintain subcriticality during cold shutdown, the reactivity increase due to temperature reduction and Xenon decay must be negated by the insertion rods. Table 2.5 tabulates the decrease in reactivity required by the reserve shutdown system for long-term shutdowns. The reactivity was then converted into the maximum K_{eff} required for a cold shutdown.

Table 2.5: K_{eff} required and reactivity increase from Xenon decay and temperature reduction in fuel and coolant to 600°K and Room Temperature (RT). The total reactivity accounts for the high limit of error at +1%.

Type	ΔT 600°K Shutdown	ΔT R.T. Shutdown	Reactivity Coefficient (pcm/K)	Reactivity 600°K (pcm)	Reactivity R.T. (pcm)
Fuel	397	728	-1.5119	613	1124
Coolant	323	733	-1.5438	499	1108*
Xeon Decay	-	-	-	2311	2311
Total	-	-	-	**3422**	**4543**
K_{eff} Required				**0.9668**	**0.9563**

*Reactivity coefficient is valid for only liquid coolant. Coolant at RT will solidify so reactivity is approximate.

Figure 2.8 displays the number of rods and the depths required to maintain long-term shutdown. Shutdown can be maintained at 600°K with a three rod system inserted more than ~35% and the four rod system with insertions greater than ~23%. Shutdown can be maintained at room temperature only with the four rod system inserted more than ~30%.

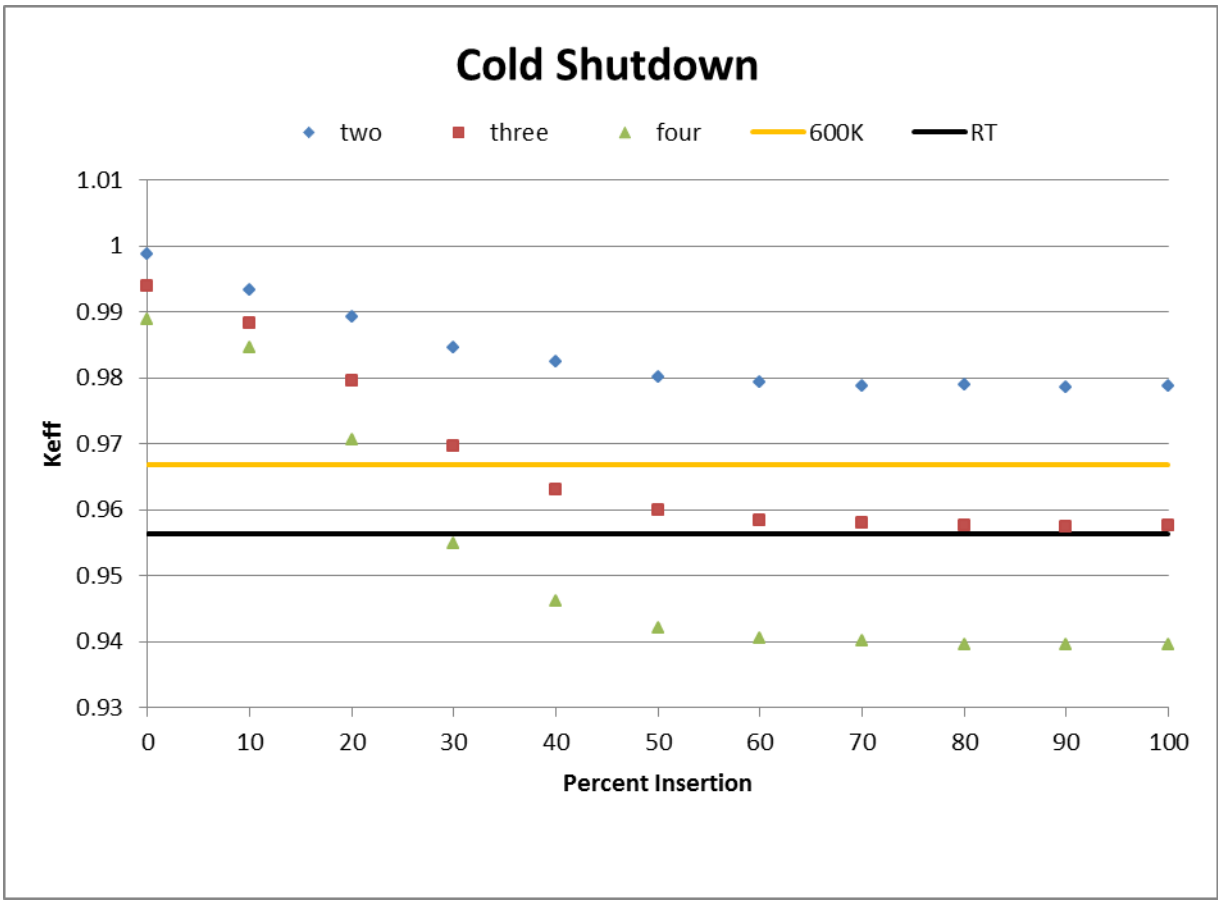

Figure 2.8: Number of rods and insertion depths required to maintain shutdown for long periods of time.

2.4 Neutronics Conclusion

The data obtained from neutronic simulations suggests that natural boron enrichment should be used for the reserve shutdown system and four rods, inserted a minimum of 30%, are required to maintain subcriticality for a cold system. Figure 2.3 implies that if cladding thickness can be reduced, the effectiveness of the shutdown system could be increased for the three rod system to become viable. The results from the scaled model advocates future analysis should be carried out to determine the effectiveness of smaller cladding rods.

3.0 MATERIALS (Justin Kong)

The shutdown rods, when inserted into the core, must withstand extreme temperature and corrosion. Two metals, molybdenum and tungsten were considered initially but ultimately, molybdenum was chosen due to its lower density and stable cost. Specifically, the molybdenum superalloy, TZM (Mo (~99%), Ti (~0.5%), Zr (~0.08%) and C (~0.03%)), will be used because it has been tested to resist molten fluoride salt at temperatures above 1300 degrees Celsius for over 1000 hours with undetectable corrosion damage (Oak Ridge 1969). Also, TZM is twice as strong as pure molybdenum and is more ductile and weldable.

Natural boron carbide will be used as the neutron poison inside the shutdown rods. Initially, the neutron poison of choice was enriched boron. However, based upon the results from MCNP simulations, it was shown that natural boron is effective enough to achieve the stable sub-criticality. The required minimum quantity of the boron will be determined by MCNP simulations by reducing the inserted amount of boron until the criticality factor is no longer acceptable. Once the required concentration of boron is determined, the remaining volume of the rods will be filled with graphite moderators.

Since the primary absorption reaction for B-10 is a (n, alpha) decay with a cross section of 3865.607 barns, approximately 99.9% of the total B-10 cross section (3868.408b), possible swelling inside the cladding must be taken into account. If the swelling occurs, the internal stress may cause buckling of the shutdown rods. In order to make the effects of swelling negligible, the shutdown rods will be placed sufficiently far away from the core.

For the scaled experimental model, the rod will be made with aluminum metal. Initially, stainless steel and aluminum metal were considered, however, it was decided that it would be easier to adjust the weight for the aluminum rod because it is lighter than stainless steel.

4.0 SHUTDOWN ROD MECHANICAL DESIGN (Shuokai Chang)

Rod geometry will significantly influence the effectiveness of the shutdown system. Because the rod is to be inserted directly into the pebble bed, it must be able to overcome the resistance caused by the fuel spheres. The geometry of the rod will determine the amount of resistance it encounters when entering the pebble bed. A smaller cross sectional area is preferred to ease the insertion of the rod. However, the required neutron absorbing material to shutdown the reactor constrains the minimum necessary size of the rod. The longitudinal shape profile of the rod must also be considered. The rod will displace a certain number of spheres, which preferably should be pushed to the side as the rod inserts rather than being pushed downward. The geometry of the rod should also aim to minimize the stresses that it exerts on the fuel spheres. Damage to the spheres is not desirable, so the rod should not exert forces that exceed the buckling strength of the spheres.

4.1 Cross Section Shape

To minimize the cross sectional area, a thin blade geometry is optimal. The exact dimensions are determined based on the pebble diameter, which is 1.27cm(0.5”) for the high density polyethylene spheres used in the experiments reported here, corresponding to 3.0 cm diameter spheres in a prototypical reactor. The blade should be under ½ pebble diameter in thickness, and 6 pebble diameters in width. Therefore, the rectangular cross section has dimensions of 0.64 cm X 7.62 cm.

The blade shape should keep the required insertion force sufficiently low. However, a shutdown blade is susceptible to buckling due to the low area moment of inertia of the thin rectangular cross section. For the cross section view shown in Figure 4.1, the area moment of inertia is calculated to be 0.17 cm^4.

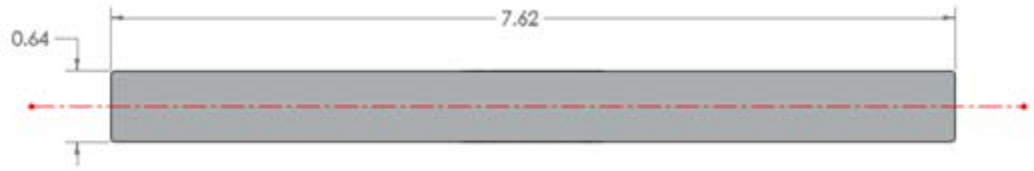

Figure 4.1: blade cross section

Flanges are added to improve the buckling strength of the rod. The cross section with flanges is shown in Figure 4.1. The area moment of inertia increases to 1.02 cm^4.

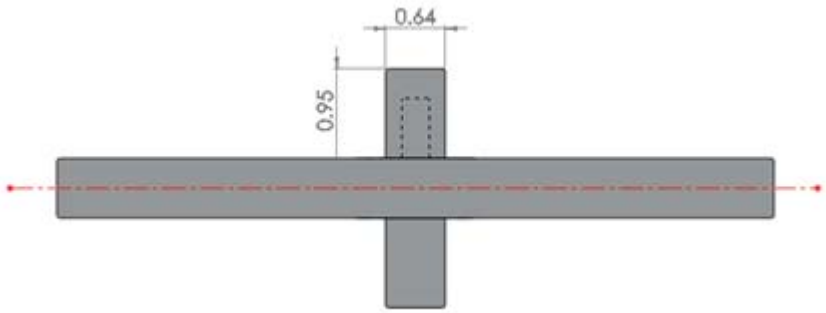

Figure 4.2: blade cross section with added flanges

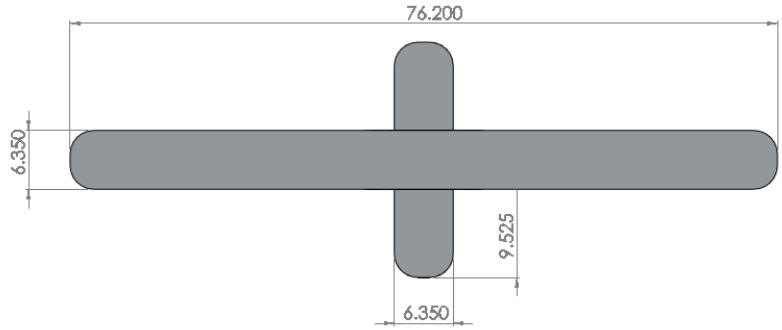

Figure 4.3: blade cross section with rounded edges; corner radius is approximately 0.03cm

4.2 Tip Profile

The tip profile is designed to minimize insertion force. Qualitative testing of the blade tips in Figure 6.2 showed that a pointed tip significantly reduces the required force. The tip has the profile shown in Figure 4.3.

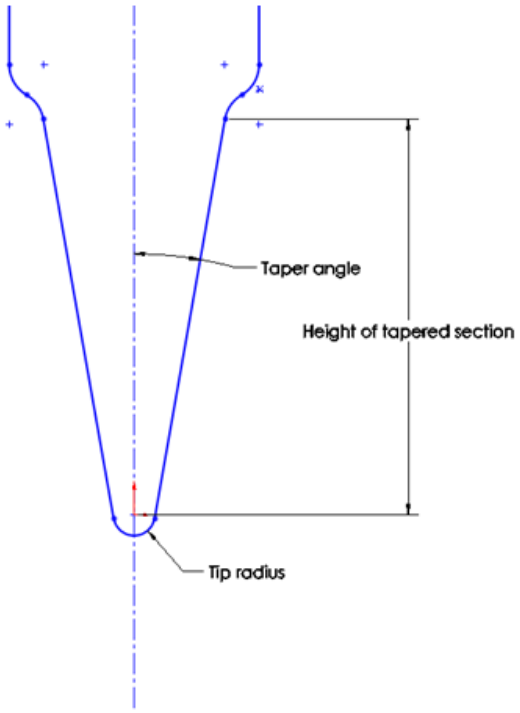

Figure 4.3: Tip profile

Several parameters can be varied to obtain the optimal profile. These are tip radius, taper angle, and height of the tapered section.

4.3 Rod Fabrication

At the current stage in the project, one rod has been fabricated for testing in a small scale pebble bed model. Four 90 degree angle bars were used cut to the appropriate profile and held together using JB Weld, a powerful metal adhesive. The procedure is shown below in Figure 4.4 and Figure 4.5

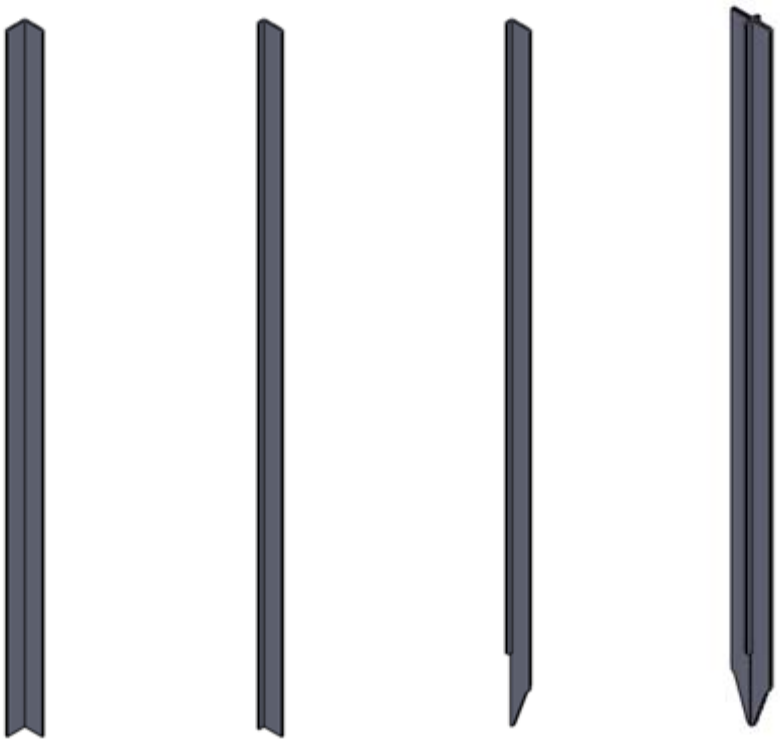

(a) (b) (c) (d)

Figure 4.4: Rod fabrication method 1. (a) 90degree angle bar. (b) One side cut to form flange (c) tip profile formed (d) 4 bars glued together

Figure 4.5: Experimental rod sections glued together with JB Weld

For future testing, several more aluminum rods will be fabricated using a different method. One blade part and two flange parts will be machined for each rod. The three parts will be attached using flathead bolts as shown below in Figure 4.6. The detailed drawings for one such rod is included in Appendix A

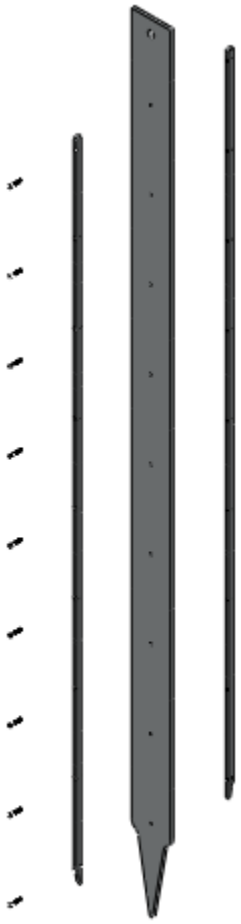

Figure 4.6: Rod fabrication method 2

5.0 MECHANISMS OF INSERTION (Abel Gonzalez)

In the case of the reserve shutdown system, the objective is to come up with a system capable of functioning independently of the remaining elements of the nuclear reactor. The reserve shutdown mechanism inserts rods of high neutron absorbing material into the nuclear reactor core to control the reactivity and bring the reactor down to subcritical conditions and maintain it there, when control rods fail to insert or bring down the reactivity due to accidental events.

When an accidental event triggers a scram signal, the shutdown rods are immediately inserted into the core by gravity. For this reason, a fast shutdown rod released mechanism is needed to quickly bring down the reactivity of the core. In PWRs and BWRs, a positioning device mechanism is used to insert the control rods into the reactor core in order to control reactivity. A similar drive mechanism can be utilized to accomplish the insertion and retrieval of

the shutdown rods in a FHR. In the case of an FHR, the drive mechanism will be located outside directly above the FHR's core.

The shutdown rod mechanism can be a system of components that operate hydraulically, electrically, magnetically, pneumatically, or by any combination of these. Or the shutdown rods can be drop by gravity into the core. The insertion of the shutdown rods can be guided by slots to facilitate the entrance to the core. A list of things such as earthquake damages, deformed guidance channels, shutdown rods getting stuck, mechanical loads, bending stresses, and normal stresses should be taking into account in order to achieve a fail-safe system.

5.1 Recommended Insertion Mechanism

To control the reactivity in an FHR, a control rod drive mechanism (CRDM) similar to the one described by Paul K. DeSantis with some modifications to meet the requirements of the FHR can be used. DeSantis describes a system comprised of a neutron absorbing device and a drive mechanism. The neutron absorbing device is a rod that serves as both, a control rod and shutdown rod.

This system is comprised by a lead screw, a motor threaded coupled with the lead to linearly insert or withdraw the rod from the reactor core, a latch assembly to the lead screw, and a release mechanism (DeSantis). In the case of an emergency when the electrical current is cut off from the electromagnetic mechanism, the latch opens and the device together with the screw are released into the core by gravity. Although, for the case of an FHR, the DeSantis CRDM would have to be modified to incorporate the materials already mentioned in this report. Figure 5.1 shows an image of the DeSantis CRDM (DeSantis).

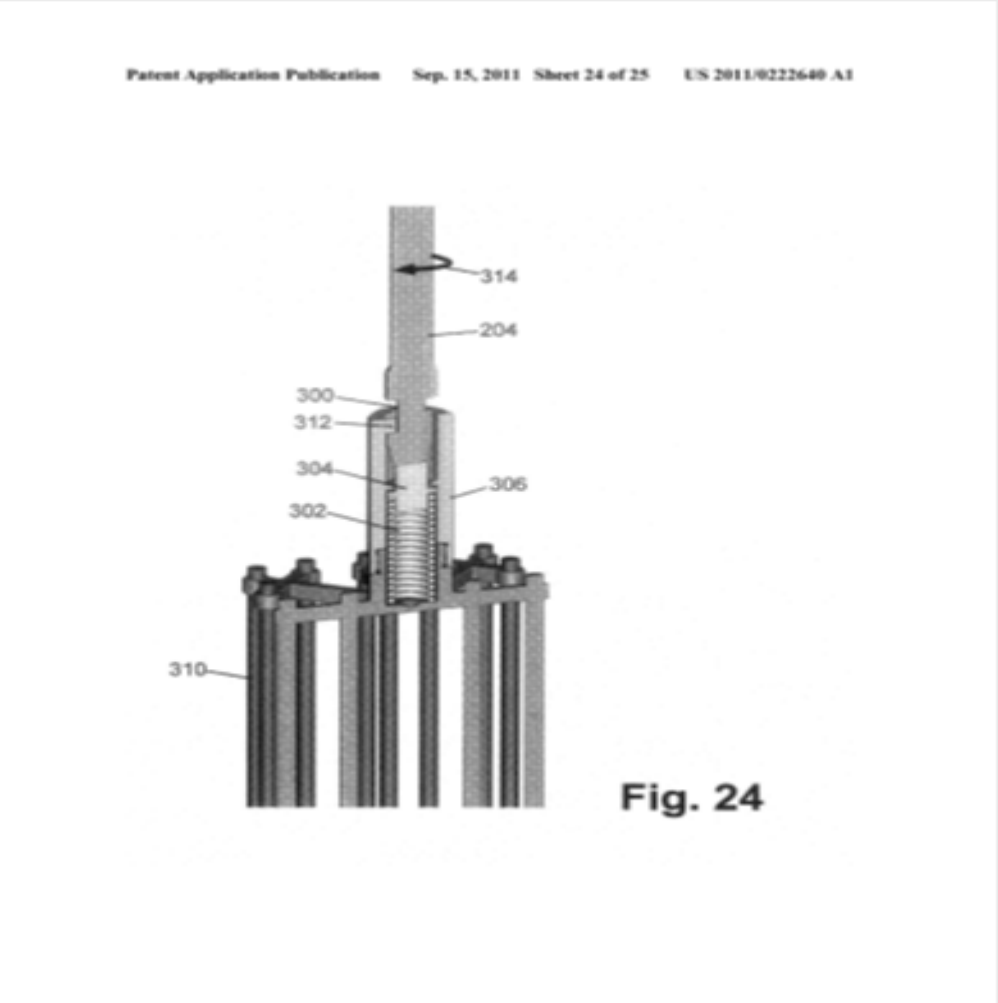

Figure 5.1: Image showing DeSantis screw type CDRM.

6.0 EXPERIMENT

6.1 Overview

The PB-FHR pebble recirculation experiment, PREX-1 (Bardet et al., 2007), was retrofitted to include scaled model of the reserve shutdown system displayed below in Figure 6.1 The system consists of an insertion mechanism and guiding system for a single shutdown rod. The dimensions of the scaled model required replacement or modification of the fuel spheres, coolant loop, converging cone, and defueling chute.

Figure 6.1: Retrofit of pebble recirculation experiment, PREX-1

The original PREX 1 experiment was scaled to model conventional 6-cm diameter helium-cooled reactor pebbles. Subsequent thermal analysis showed that 3-cm pebbles can enable higher power density operation. The reserve shutdown rod was modified to use smaller fuel spheres and the blade was designed to have a width of six pebble diameters. The coolant loop was also rebuilt to accommodate the new pebble size, and now includes a pebble injection system consisting of a hopper feeding pebbles into the coolant loop following the fluid pump.

The converging cone was modified to accommodate insertion of the shutdown rod into the pebble core by cutting a cross-sectional projection of the rod into the cone. Because the cone was originally designed to include larger fuel spheres, netting was fixed to the inner surface of the cone to prevent the new ½" diameter pebbles from pinning in the holes and getting stuck during defueling.

The rod insertion and guiding system was designed for consistent testing. Insertion of the rod was carried out by a pulley system via a rope attached to the top of the rod. The rope was then hoisted to a specific height and released for insertion. The stopping mechanism consisted of tying the rope off at a specific length so that rod tip does not impact the bottom of the tank during insertion. The guiding mechanism consisted of plastic block bolted to the defueling chute

flange. The block was hollowed out in the shape of the shutdown rod to prevent the rod from crooked insertion.

6.2 Procedure

Although there was only one rod out of three available to test, the following will describe an appropriate procedure for the reserve shutdown model experiment. It was determined that a total of six experimental groups would be required for this experiment. Therefore, this experiment involves six experimental groups. Each experimental group consisted of two controlled variables (aluminum blade and packed bed), one independent variable (flow rate), and one dependent variable (weight required to fully insert the blade into the packed bed).

The packed core of a prototypical reactor was represented by the amount of High Density Polyethylene (HDPE) spheres of 1.27 cm (0.5 inch) diameter that occupy a given volume at the top of the Pebble Recirculation Experiment (PREX-1). PREX-1 was retrofitted for the blade insertion experiment and is described in section 6.1 of this report. There are two blades with dimensions 0.635 X 7.62 X 152.4cm (0.25”X3”X5’), and one blade with dimensions 0.635 X 7.62 X 152.4cm (0.25”X3”X4’). All three blades are made of 6061 aluminum. To strengthen the blades, flanges with dimensions of 0.9525cm X 0.635cm (0.375”X0.250”) were added along the 7.62cm (3 inch) side of the blades. Each blade weighs about 2.24 kg (5 lbs) and has one taper end with tip radius of 0.3175 cm (1/8 inch), 0.635 cm (1/4 inch), or 1.27 cm (1/2 inch). The height of each tapered end is 12.7cm (5 inches).

A water pump capable of producing different flow rates was connected to PREX-1 in a closed loop. Water will serve as the coolant in this model and represents the coolant salt of a prototypical reactor. The water pump was set at different flow rates from 0.0 to 50 gpm in this experiment. For each of the set flow rates, a single blade was inserted different times into the pebble bed to determine the amount of weight needed for full insertion.

The blade was attached to a release mechanism and aligned with the guiding mechanism. This insured the blade to enter the opening on the 45 degree cone of PREX-1, when released from the release mechanism. The driving force on the blade after it is released will be gravitational force. The release mechanism was located outside and above PREX-1. It was desired to repeat this process six times, one time for each experimental group. Each run was recorded to obtain a time vs depth relationship and to determine the minimum time required to fully insert the blade. Standard weights of 1.14 kg (2.5 lbs) in the form of disks were used to determine the minimum weight required to fully insert the blades into the packed bed. These standard weights were placed on an extended section of the blade attached to the top of the blade. The amount of weight added to the top of the blade to fully insert it plus the weight of the blade for each experimental group, will be used to determine the minimum force needed to fully insert the blade into the pebble bed. Ideally, the insertion of the blade should be without deforming or fracturing the spheres or the blade itself.

The following materials were needed to conduct the reserve shutdown rod experiment: A Pebble Recirculation Experiment (PREX-1), a water pump capable of producing different flow rates connected to PREX-1 in a closed loop, High Density Polyethylene (HDPE) spheres of 1.27 cm (1/2 inch) diameter to form the packed bed at the top of PREX-1, 3 aluminum blades with different tip radii, release mechanism to release the blades from above PREX-1 (pulley and

rope), guide mechanism to guide the blades into the packed bed, standard weights of 1.14 kg (2.5 pounds), some kind of measuring tape, and a video recorder.

A step by step procedure to perform the shutdown rod experiment is described below.

1. Label one side of each blade with a measuring tape to determine the depth of the blades as a function of time as the blades moves down the packed bed.

2. Number the blades from 1-3 based on their tip radius.

3. Add HDPE spheres to PREX-1 from the top to obtained the desired packed bed, then add water to allow the HDPE spheres to collect at the top and form the packed bed.

4. Turn on the water pump and set the desired first flow rate.

5. Attach blade 1 to the release mechanism and align the blade with the guiding mechanism, so that when released, the blade enters the opening on the 45 degree cone of PREX-1.

6. Release blade 1 from the attachment and record the depth of the blade as a function of time with the video recorder, as the blade moves down the packed bed.

7. Repeat steps 5 and 6, and gradually increase the amount of weight on top of blade 1 to allow the blade to fully insert into the packed bed with the least amount of weight needed.

8. Change the flow rate and repeat steps 5, 6, and 7 above for all desired flow rates.

9. Repeat steps 5, 6, 7, and 8 above for blades 2 and 3.

10. Change the packed bed value by adding more HDPE spheres and repeat steps 5, 6, 7, 8, and 9 above.

These above steps are shown in table 6.2 below to show the relationship between the experimental groups, the controlled variables, the independent variable, and the dependent variable.

Table 6.2 Experimental Procedure

		Controlled Variable	Controlled Variable	Independent Variable	Dependent Variable
Experimental group	Run/Trial number	Packed bed value, 1 or 2	Blade with tip 1, 2, or 3	Vary the flow rates by 10 gpm	Weight required to

				from 0-50 gpm	fully insert the blade
1	1-6	1	1	Value 1-6	
2	7-12	1	2	Value 1-6	
3	13-18	1	3	Value 1-6	
4	19-24	2	1	Value 1-6	
5	25-30	2	2	Value 1-6	
6	31-36	2	3	Value 1-6	

Figure 6.2: Test blade with blunt end on left and pointed end on right. The Blunt end should need greater force to insert due to the larger surface area causing higher friction forces, and the pointed end should need less force to insert due to smaller surface area.

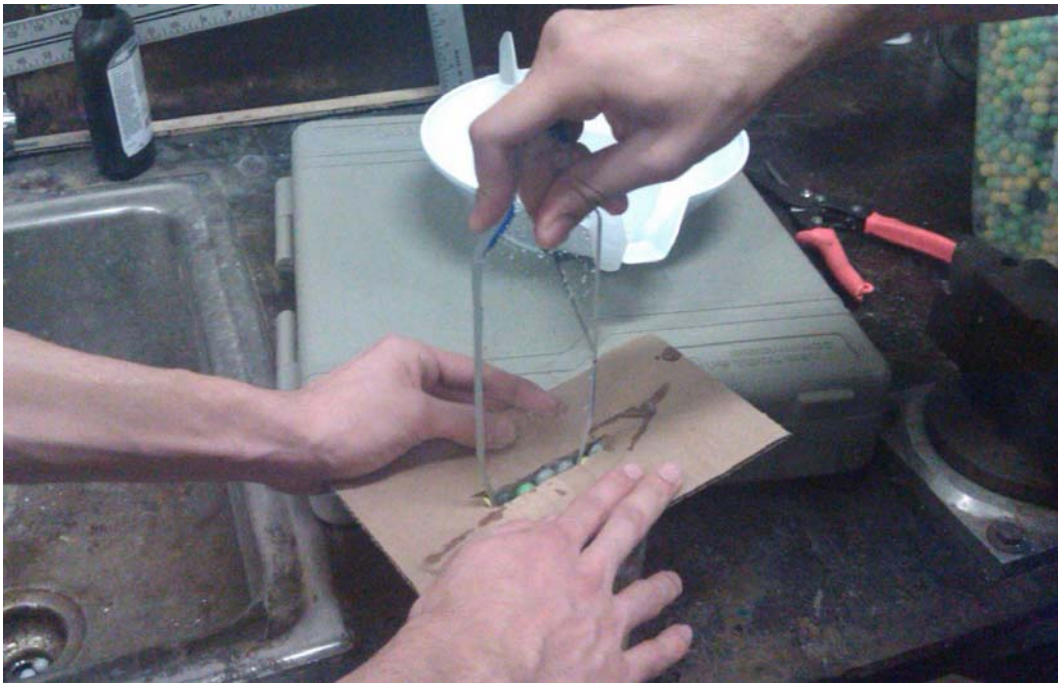

Figure 6.3: Insertion test of blunt end of blade into packed bed of spheres.

Figure 6.4: Insertion test of pointed end of blade into packed bed of spheres.

Figure 6.5: Blunt end tends to pin spheres during insertion which could cause rupture of fuel pebbles on impact.

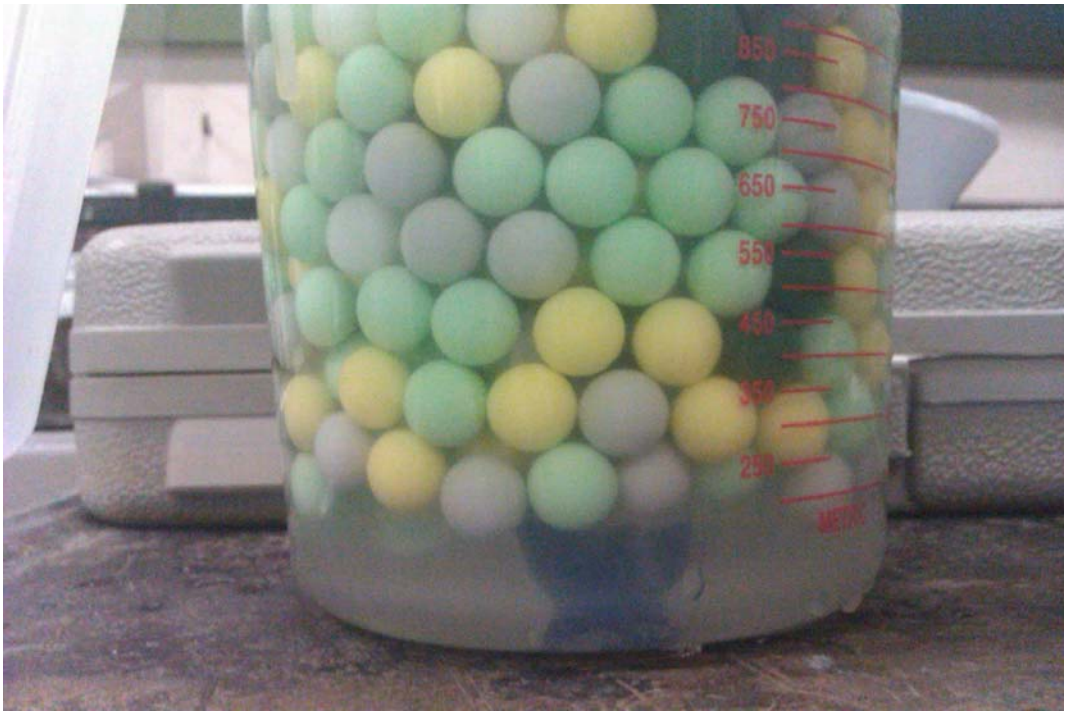

Figure 6.6: Pointed end of test blade did not pin spheres during any of the insertion tests.

6.3 Experimental Results

The results of our initial rod profile design testing were shown in the pictures above. The blunt-tip design risks damaging the spheres by pinning them down while the pointed-tip design is less likely to have the same problem.

PREX-1 testing showed that our makeshift aluminum rod inserted into the pebble bed without any problems, additional weights were not necessary for any flow rates tested or for the packed bed scenario. Figure 6.7 and Figure 6.8 show the fully inserted rod in the unpacked and packed cases respectively.

Figure 6.7: Full rod insertion into unpacked core.

Figure 6.8: Full rod insertion into packed core before (right) and after (left).

The effects of water flow in the PREX-1 tank on the efficiency of the rod insertion were negligible. Upon examination, the difference in the time the rod takes to be fully inserted varied about two-tenth of a second between a 10 gallons per minute flow and 40 gallons per minute flow. Such result is not significant enough to be considered in depth for the purpose of our experiment.

6.4 Experimental Conclusion

The testing thus far suggests that the proposed rod design meets the necessary criteria. Insertion of the rod is fast and requires very little force. The weight of the rod alone is enough to drive it into a packed pebble bed. There is no visible deflection or bending of the rod, and no spheres are damaged. Increasing the flow rate of coolant through the core somewhat hinders the insertion speed, however, this effect is not significant.

6.5 Suggestions for Future work

Other tip profiles should be tested to determine the optimal profile. A test with a completely blunt tip might also be beneficial to establish a baseline. In the tests done thus far, the packed bed had a height that was less than the length of the rod, and the tip of the rod impacted the bottom of the vessel. In the future, the height of the packed bed should be increased to determine the maximum depth to which the rod can be inserted under its own weight.

7.0 REFERENCES

P. Bardet, J.Y. An, J.T. Franklin, D. Huang, K. Lee, M. Toulouse and P.F. Peterson, "The Pebble Recirculation Experiment (PREX) for the AHTR," proceedings of Global 2007, Boise, Idaho, September 9-13, 2007, pp. 845-851.

Blandford, Edward David. "Report UCBTH-003." Risk-informed Design Guidance for Advanced Reactor Concepts: A Case Study of the Pebble Bed Advanced High Temperature Reactor. University of California Berkeley, Spring 2008. Web. 2 Mar 2012. <http://pb-ahtr.nuc.berkeley.edu/papers/08-033_Blandford_Masters_Report.pdf>.

DeSantis, Paul K. "CONTROL ROD DRIVE MECHANISM FOR NUCLEAR REACTOR." United States Patent Applicaion Publication DeSantis 15 Sep. 2011. Google Patents. Web. 22, April 2012. <http://www.google.com/patents?id=jBLuAQAAEBAJ&pg=PA5&dq=scram+%2B+magnetic&source=gbs_selected_pages&cad=2#v=onepage&q=scram%20%2B%20magnetic&f=false>.

Oak Ridge National Laboratory Report. Compatibility of Molybdenum-Base Alloy TZM, with LiF-BeF2-ThF4-UF4". 1969-12. Retrieved 2010-09-02.

APPENDIX A

ROD 1
NE 170
Draw by Shuokai Chang
4/24/12
Not to Scale
All dimensions to ± 1/16"

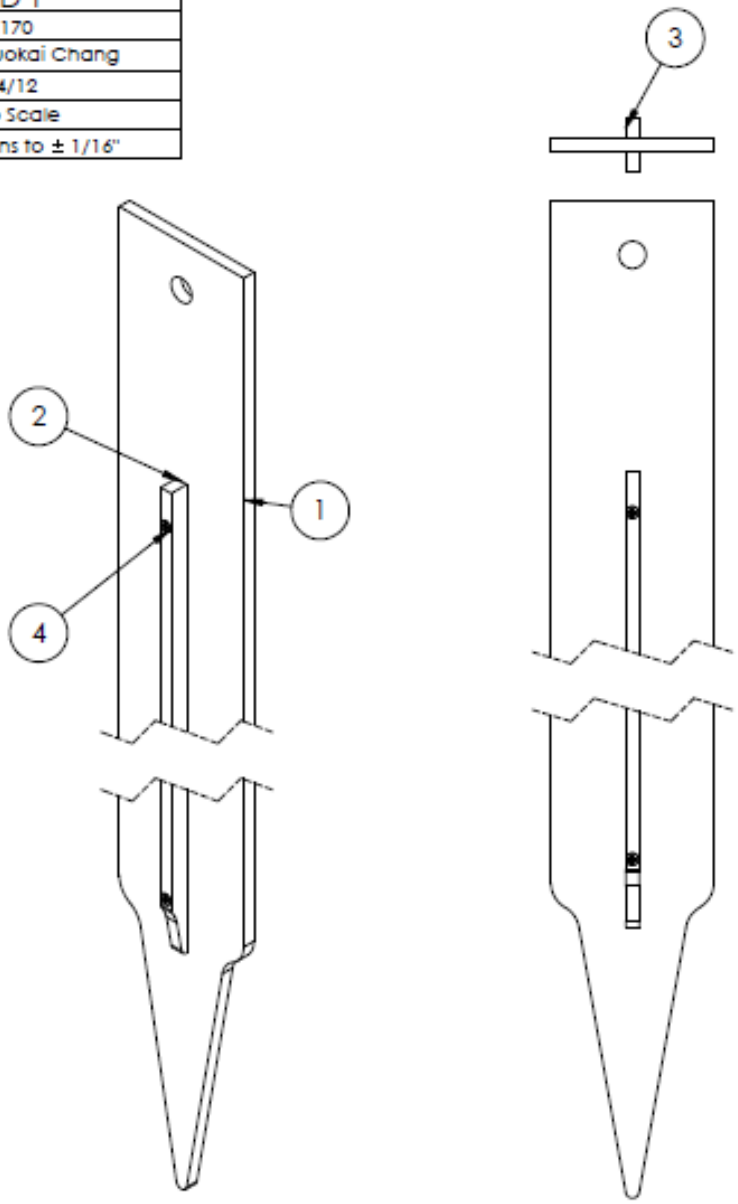

ITEM NO.	PART	DESCRIPTION	QTY.
1	Blade1		1
2	Flange1	Countersunk through holes	1
3	Flange2	4-40 thread tapped holes	1
4	Screw	4-40X7/8 through all three other parts	9

BLADE 1
NE 170
Draw by Shuokai Chang
4/24/12
Not to Scale
All dimensions to ± 1/16"

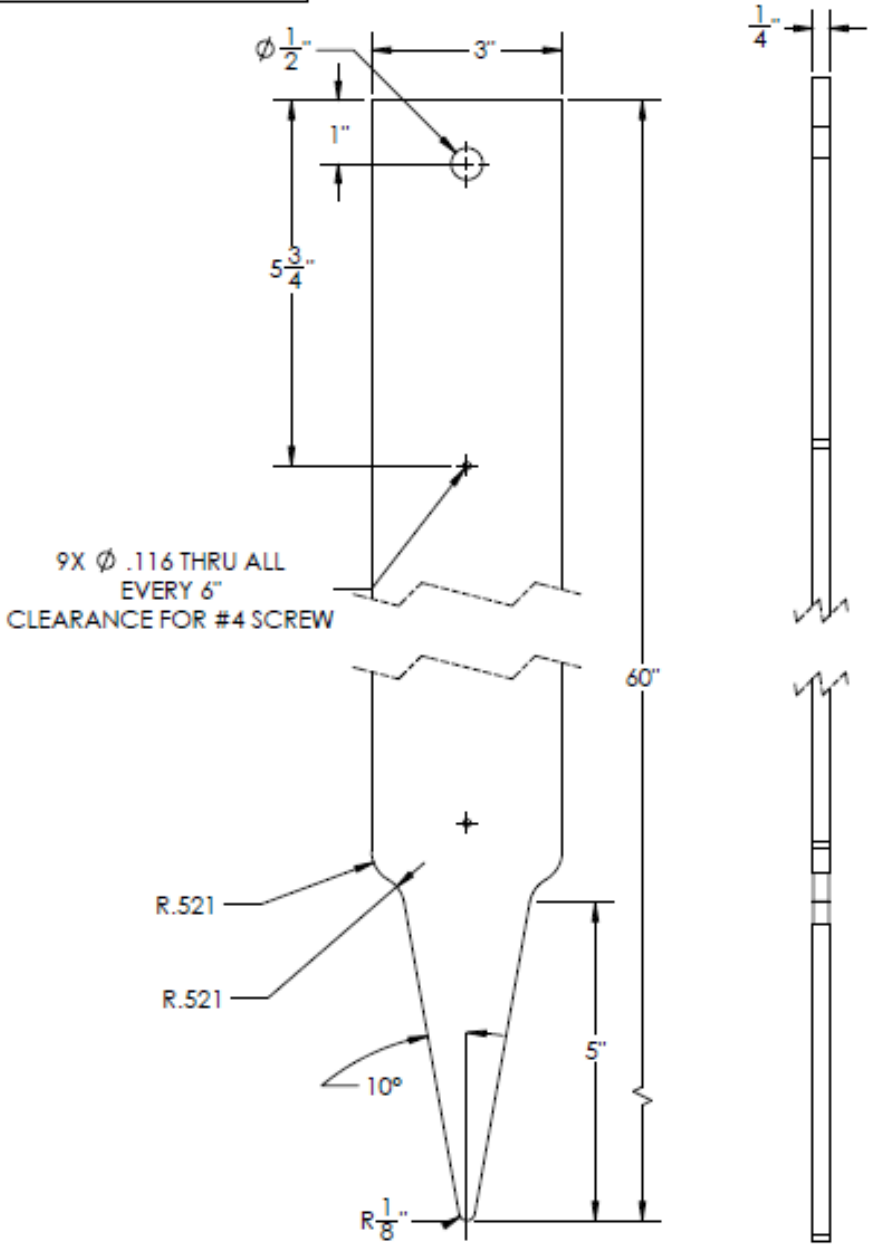

FLANGE 1
NE 170
Draw by Shuokai Chang
4/24/12
Not to Scale
All dimensions to ± 1/16"

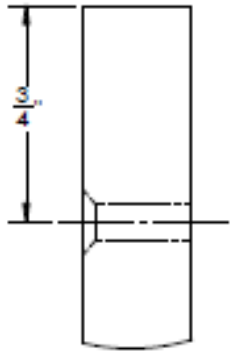

DETAIL B
SCALE 2 : 1

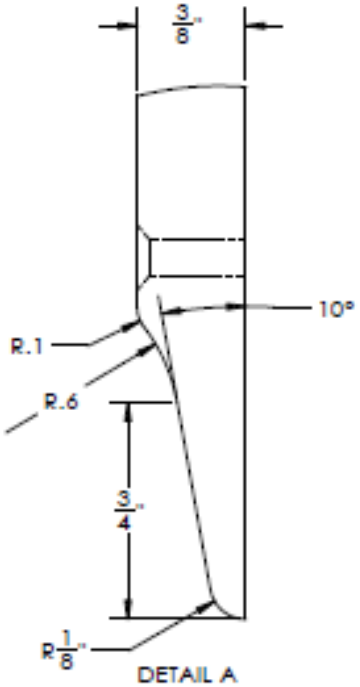

DETAIL A
SCALE 2 : 1

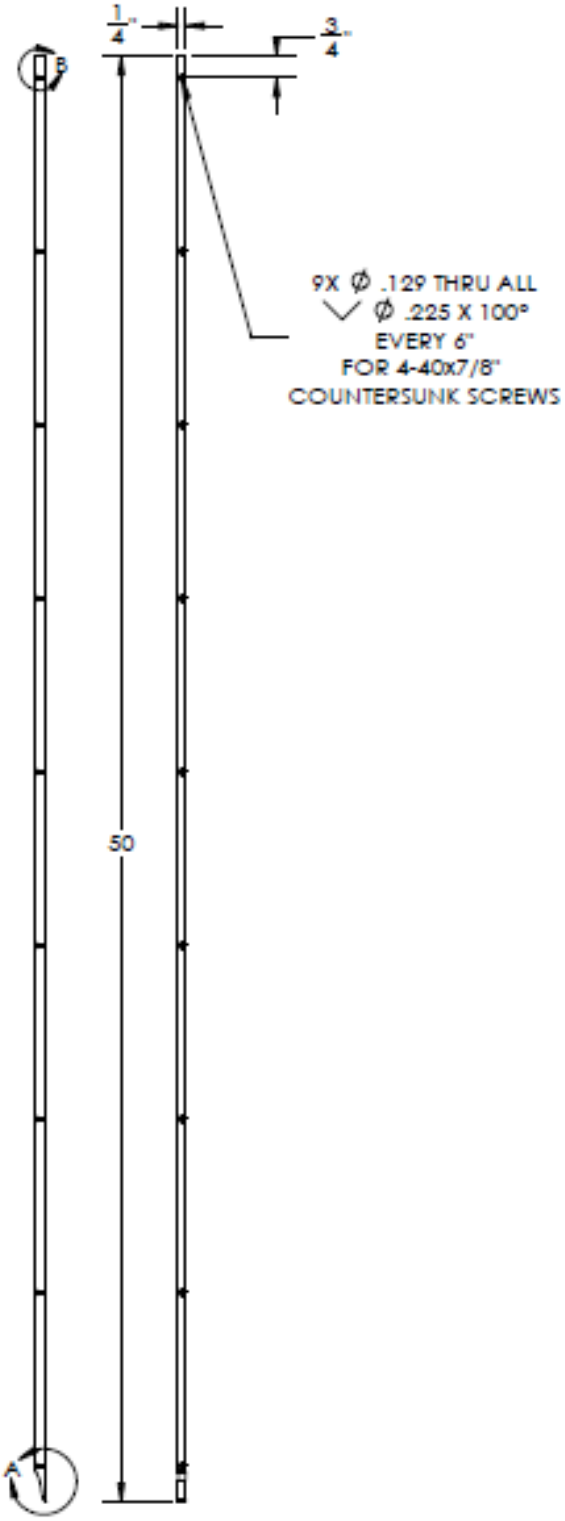

FLANGE 1
NE 170
Draw by Shuokai Chang
4/24/12
Not to Scale
All dimensions to ± 1/16"